

NUCLEAR SHADOWING IN NEUTRINO DEEP INELASTIC SCATTERING ¹

S. A. Kulagin

Institute for Nuclear Research, Russian Academy of Sciences, Moscow, Russia

E-mail: kulagin@ms2.inr.ac.ru

Abstract

We discuss effect of nuclear shadowing in neutrino deep-inelastic scattering in terms of non perturbative parton model. We found that for small Bjorken x and large Q^2 the structure function F_3 is shadowed in nuclei about two times as stronger as F_2 . The underlying reason and phenomenological aspects of this observation are discussed.

Key-words: neutrino, deep inelastic scattering, nuclear effects, nuclear shadowing

1 Introduction

The small x physics is an important topic of high energy studies nowadays. We note in this respect that data is usually collected for nuclear targets and it is important to consider nuclear effects in deep inelastic scattering (DIS). The systematic reduction of the nuclear structure functions F_2^A/A with respect to the nucleon F_2^N has been established experimentally at CERN [1] and Fermilab [2] in the region of small Bjorken x , so called nuclear *shadowing* phenomenon. This phenomenon has been extensively discussed in the literature within different theoretical approaches (for a review see ,e.g., ref.[3]).

Apart from F_2 , it is important of course to study the nuclear effects in the other observed structure functions. An interesting object in this respect is the structure function F_3 which is measured in (anti)neutrino DIS. We recall that at large momentum transfer F_3 describes the valence quark distribution in the target. The main concern of the present paper is to study the nuclear effects in neutrino DIS in the small x region and compare the shadowing effect for the structure functions F_2 and F_3 , i.e. for the sea and the valence quark distributions.

For the discussion of nuclear physics at DIS it is convenient to choose the target rest frame. To clarify the space-time picture of DIS in this reference frame it is convenient to argue using the time-ordered ('old') perturbation theory. We recall that DIS cross section is determined by the imaginary part of the Compton scattering amplitude of the virtual intermediate boson from the target. Two typical time-ordered diagrams which contribute to the Compton nucleon scattering amplitude are drawn in Fig.1.



FIG.1

Time-ordered diagrams ($t_1 < t_2$) for the Compton scattering.

¹ Based on the talk given at XIV International Seminar 'Relativistic Nuclear Physics And Quantum Chromodynamics' Dubna, August 17-22, 1998. To be published in proceedings.

Fig.1a describes the scattering process which goes via absorption and re-emission of the virtual boson by a quark bound in the target. Fig.1b shows the process where the virtual boson first decays into a $q\bar{q}$ -pair which then interacts with the target. By comparing the energy denominators of these two diagrams one can observe that at small x the diagram in Fig.1b dominates over the one in Fig.1a. This observation leads to the qualitative space-time picture of the Compton scattering at small x which consists from two time-ordered processes. First, the virtual boson splits into a $q\bar{q}$ (or hadronic) fluctuations before arrival at the target. Then these states propagate and interact with the target. A typical propagation length of a $q\bar{q}$ fluctuation can be estimated from the uncertainty principle and at high Q^2 is of order $L \sim (2Mx)^{-1}$ with M the nucleon mass² [4]. For $x \ll 0.1$ the $q\bar{q}$ fluctuation lives long enough to develop a chain of multiple interactions with bound nucleons. This will lead to nuclear shadowing effect which we discuss in detail in Sec.3. Before we come to the discussion of nuclear modifications in the DIS, in Sec.2 we set up the model for the DIS from the isolated nucleon and fix some parameters of the model by comparing to data.

2 DIS in non perturbative parton model

We consider the neutrino and antineutrino charged-current DIS from the nucleon. It is supposed that Q^2 is sufficiently high to neglect the target mass effects. We neglect also possible final state interaction effects and focus on the leading twist contribution to the DIS which is given by the handbag diagram of Fig.2 (note that this diagram is treated in terms of a covariant approach which includes of course all time-ordered processes shown in Fig.1).

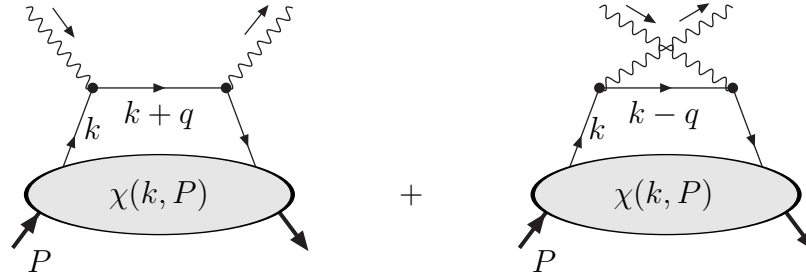


FIG.2

Compton scattering amplitude from the nucleon to the leading order in Q^2 .

In the axial gauge the Compton amplitude for the scattering of virtual W -boson from the target reads (to be specific we consider the Compton scattering of W^+ -boson):

$$T_{\mu\nu}(P, q) = -i \int \frac{d^4k}{(2\pi)^4} \text{Tr} \left[\chi_d(k, P) \gamma_\mu (1 + \gamma_5) (\not{k} + \not{q} + i\epsilon)^{-1} \gamma_\nu (1 + \gamma_5) + \chi_u(k, P) \gamma_\nu (1 + \gamma_5) (\not{k} - \not{q} + i\epsilon)^{-1} \gamma_\mu (1 + \gamma_5) \right] + \dots, \quad (1)$$

where q is momentum transfer and $\chi_a(k, P)$ is the propagator of the quark fields of kind a in the target with momentum P ,

$$\chi_a(k, P) = -i \int d^4\xi e^{ik \cdot \xi} \langle P | T (\psi_a(\xi) \bar{\psi}_a(0)) | P \rangle. \quad (2)$$

² L is also a typical time between absorption and emission of the virtual boson in Fig.1

The dots in Eq.(1) denote contributions from the s - and c -quarks which repeat the first two terms with the substitutions $u \rightarrow c$ and $d \rightarrow s$.

The structure functions are given by the imaginary part of the Compton amplitude and can be found from Eq.(1) by applying appropriate projection operators. In the leading order in $1/Q^2$ we find that the structure functions F_2 and F_3 are given in terms of the quark light-cone distributions by the standard parton model equations (neglecting a small effect due to Cabibo mixing angle),

$$F_2^\nu(x) = 2x(d(x) + \bar{u}(x) + s(x) + \bar{c}(x)), \quad (3)$$

$$F_3^\nu(x) = 2(d(x) - \bar{u}(x) + s(x) - \bar{c}(x)). \quad (4)$$

where the parton distributions are expressed in terms of the quark propagator as follows,

$$f_a(x) = -i \int \frac{d^4k}{(2\pi)^4} \frac{\text{Tr}(\not{q} \chi_a(k, P))}{2P \cdot q} \delta\left(x - \frac{k \cdot q}{P \cdot q}\right), \quad (5)$$

$$q_a(x) = f_a(x), \quad \bar{q}_a(x) = -f_a(-x). \quad (6)$$

Note that the quark and antiquark distributions come from the direct and the crossed terms of the Compton amplitude respectively. It follows from Eq.(1) that the structure function F_1 is not independent; it is given by the Callan-Gross relation, $F_2(x) = 2x F_1(x)$.

In QCD scaling is violated and the parton distributions depend also on Q^2 . The Q^2 dependence comes through the dependence of the quark correlator on the normalization point μ^2 which is taken to be Q^2 in our discussion.

For our purposes it will be convenient to write the parton distributions as the integrals over the invariant mass spectrum of the spectator states [5]. To this end we assume the analytic properties of the quark correlator (2) to be similar to the ones of hadronic amplitudes, i.e. it is an analytic function of the invariant variables $s = (P - k)^2$, $u = (P + k)^2$ and k^2 . For real s and u the quark amplitude has a right-hand cut in the variable s , a left-hand cut in the variable u and singularities at $k^2 > 0$. In order to make use of these analytical properties of in the loop integral (5), it is convenient to parameterize the loop momentum k in terms of the light-cone or the Sudakov variables. Acting along these lines one finds that the distribution function $f(x)$ vanishes outside the physical interval $|x| \leq 1$. For $0 \leq x \leq 1$ the distribution function $f(x)$ (or the quark distribution $q(x)$) is given by a dispersion integral along the cut in the s -channel, while for $-1 \leq x \leq 0$ the u -channel cut is relevant. We separate from the quark correlator (2) external quark propagators and write the result in terms of the quark-nucleon, T_{qN} , and the antiquark-nucleon, $T_{\bar{q}N}$, scattering amplitudes. In terms of these amplitudes the small x part of the quark and antiquark parton distributions read as follows (to simplify notations we drop here explicit dependence on the quark kind a)

$$q(x) = \frac{N_c}{(2\pi)^3} \int ds \int^{k_{\text{max}}^2(s,x)} dk^2 \frac{\text{Im} T_{\bar{q}N}(s, k^2)}{(k^2 - m_q^2)^2} \left(-x + \frac{m_q^2 - k^2}{s - M^2 - k^2}\right), \quad (7)$$

$$\bar{q}(x) = \frac{N_c}{(2\pi)^3} \int du \int^{k_{\text{max}}^2(u,x)} dk^2 \frac{\text{Im} T_{qN}(u, k^2)}{(k^2 - m_q^2)^2} \left(-x + \frac{m_q^2 - k^2}{u - M^2 - k^2}\right). \quad (8)$$

Here N_c is the number of colors, m_q is the quark mass. The integrations run over the spectrum of intermediate states and over the quark four-momentum squared k^2 with $k_{\text{max}}^2(s, x) = x(M^2 - s/(1 - x))$ being the kinematical maximum of k^2 for the given s

and x . We note that the quark distribution $q(x)$ is determined by the $\bar{q}N$ -scattering amplitude, in accordance with intuitive discussion based on time-ordered diagrams of Fig.1. For the antiquark distribution $\bar{q}(x)$ the qN -amplitude is relevant. The reader can find the derivation of Eqs.(7,8) in ref.[6].

Eqs.(7,8) establish the correspondence between the x -dependence of parton distributions and the region of invariant masses of the residual quark system. The basic assumption of the non-perturbative parton model is that the parton amplitudes vanish at large virtualities so that the integrals in Eqs.(7,8) are finite and saturated in the region of finite k^2 . At small x the k^2 is finite even for large $s \sim M^2/x$ and therefore the parton distributions are sensitive to the large- s part of the spectral densities.

In ref.[6] (see also [7]) we have considered a simple model for the spectrum of the residual quark system which incorporates two scattering mechanisms shown in Fig.1. It was assumed that the spectrum of spectator states is divided into low-mass and high-mass parts sharply at some separation parameter s_0 . The physical origin of the low-mass part of the spectrum is due to the Compton scattering of the intermediate boson from bound quarks in the target, Fig.1a. This process is of major importance at intermediate and large x . The high-mass part of the spectrum ($s > s_0$) gives rise to the low- x part of the structure functions. In this region the spectrum is dominated by the process shown in Fig.1b.

In order to calculate the quark and anti-quark distributions one has to specify the amplitudes T_{qN} and $T_{\bar{q}N}$. We follow here ref.[6] and extract the quark-nucleon amplitudes from the observed high-energy hadron scattering amplitudes. The idea is to approximate the amplitudes T_{qN} and $T_{\bar{q}N}$ by the constituent quark-target scattering amplitudes which we obtain from the additive quark model of high-energy scattering. We are concerned here with the scattering from the isoscalar target. The isoscalar parts of the (anti)proton-nucleon forward scattering amplitudes, $T_{pN} = (T_{pp} + T_{pn})/2$ and $T_{\bar{p}N} = (T_{\bar{p}p} + T_{\bar{p}n})/2$, can be written in terms of the (anti)quark-nucleon amplitudes as,³

$$\begin{aligned} T_{pN}(S)/S &= \langle T_{qN}(yS, k^2)/yS \rangle, \\ T_{\bar{p}N}(S)/S &= \langle T_{\bar{q}N}(yS, k^2)/yS \rangle. \end{aligned} \quad (9)$$

Here S is the nucleon-nucleon invariant mass squared, k is the four-momentum of a constituent quark in the target and y is a fraction of the target light-cone momentum carried by the constituent quark. The averaging is taken over the quark distributions in the proton which is normalized to the number of quarks.

An approximate solution of Eqs.(9) can be obtained by evaluating the qN and $\bar{q}N$ amplitudes at averaged values of y and k^2 for constituent quarks in the proton, $\bar{y} \sim 0.2$, $\bar{k}^2 \sim -0.3 \text{ GeV}^2$. The s -dependence of the (anti)quark amplitudes is then fixed by the energy dependence of the observed pN and $\bar{p}N$ scattering amplitudes. In the Regge approach these amplitudes can be approximated by the exchange of the Pomeron P and two Regge poles corresponding to the scalar (f) and the vector meson (ω) trajectories [8], $T_{pN} = P + f - \omega$, $T_{\bar{p}N} = P + f + \omega$. Eqs.(9) thus determine the quark-nucleon Regge poles residues in terms of the nucleon-nucleon ones. The exchange of the Regge trajectory with the intercept α_R leads to the imaginary parts of the amplitudes rising as s^{α_R} . The

³ In fact if the isospin is the exact symmetry one finds $T_{uN} = T_{dN} = T_{qN}$ and $T_{\bar{u}N} = T_{\bar{d}N} = T_{\bar{q}N}$. We have used this observation implicitly by writing Eq.(9) in terms of only two isoscalar quark-nucleon amplitudes.

Pomeron exchange dominates both $q(x)$ and $\bar{q}(x)$ at small x which rise asymptotically as $x^{-\alpha_P}$, as one can see from Eqs.(7,8). The Pomeron and the scalar f -Regge pole cancel out in the difference $q - \bar{q}$ (the valence quark distribution). Note however that the valence quark distribution remains finite at small x with the asymptotics determined by the ω Regge trajectory, $q(x) - \bar{q}(x) \sim x^{-\alpha_\omega}$. In the numerical estimates we use the parameters of best fit of ref.[9] with the Regge poles intercepts $\alpha_P = 1.08$ and $\alpha_f = \alpha_\omega = 0.55$.

In the model of ref.[6] it is assumed that the coupling of the Regge poles to quarks is independent of its kind, and thus the different parton distributions are described by two amplitudes T_{qN} and $T_{\bar{q}N}$.⁴ In order to have the integrals in Eqs.(7,8) convergent the amplitudes should fall sufficiently fast for large quark virtualities k^2 . We assume the factorized s - and k^2 -dependencies for every Regge pole in the quark-nucleon amplitude which we parameterize in a simple form $(1 - k^2/\Lambda_R^2)^{-n_R}$. The cut-off and exponent parameters as well as the scale parameter s_0 of the spectrum of spectator states are chosen to fit the charged-lepton and neutrino data for the structure functions F_2 and xF_3 at average momentum transfer Q^2 between 5 and 10 GeV² (for more details see ref.[6]).

A comment on the scaling violation is in order. In our approach we fix the parameters of the spectrum of spectator states to describe the measured structure functions at some fixed Q^2 and therefore effectively incorporate the Q^2 evolution effect in the phenomenological parameters of the spectrum. A more consistent approach which accounts for the scaling violation effect would be to choose a low resolution scale, $Q^2 \sim 1$ GeV², and fix the parameters of the spectrum at this scale. Then at larger Q^2 the parton distributions are obtained by applying the Q^2 evolution equations. This program in fact has been attempted in ref.[7].

3 Nuclear Shadowing

We now turn to discussion of DIS on nuclear targets in the small x region. The physical origin of nuclear corrections in the small x region is the coherent interaction the propagating $q\bar{q}$ pair with bound nucleons. In the parton model regime, which is discussed in this paper, the $q\bar{q}$ pair is highly asymmetric in the target rest frame, i.e. one of the pair constituents carries practically all the transferred momentum. It is commonly assumed that the fast quark only weakly interacts with the target and begins to radiate soft gluons and hadronize well after the nucleus. The other participant, the wee (anti)quark, has a finite momentum and interacts in the nucleus with normal hadronic cross-section.

It is instructive to compare different time and length scales involved in this process. The onset point of coherent nuclear effects x_o is usually estimated by the comparison of the propagation length $L \sim (2Mx)^{-1}$ of the $q\bar{q}$ pair with the averaged distance between bound nucleons in the nucleus. If we take for estimates the averaged nuclear density $\rho = 0.17$ fm⁻³ in the central nuclear region then $x_o \approx 0.1$. We note however that this is only a kinematical condition which allows for coherent interactions of the propagating $q\bar{q}$ pair with several nucleons for $x < x_o$. It is quite clear that the region of developed nuclear shadowing should depend on (anti)quark-nucleon interaction. Indeed if σ is the averaged (anti)quark-nucleon total cross section then the (anti)quark mean free path in the nucleus $l = (\rho\sigma)^{-1}$. The multiple scattering effect becomes significant when the

⁴ We note in this respect that the parton distributions depend on their masses, as one can see from Eqs.(7,8). Therefore the contribution from heavy quarks is suppressed by their large masses.

coherence length L exceeds the (anti)quark mean free path in the nucleus l . This happens when $x < \rho\sigma/2M \approx 0.02$, where we have taken for estimates $\sigma = \sigma_{pp}^{tot}/3 \approx 13$ mb. In this case the main part of the incoming flux of $q\bar{q}$ pairs is absorbed at the nuclear surface in the layer with the thickness of order l and thereby the inner nucleons are screened.

In order to quantify the discussion we consider the quark and antiquark nuclear scattering amplitudes in forward direction, T_{qA} and $T_{\bar{q}A}$, and apply the Glauber-Gribov multiple scattering expansion [10, 11] assuming that formalism can be taken over to off-shell interaction,

$$T_A = AT_N + \delta^{(2)}T_A + \dots \quad (10)$$

$$\frac{i\delta^{(2)}T_A(s, k^2)}{2s} = A(A-1) \left(\frac{iT_N(s, k^2, t)}{2s} \right)^2 \int_{z' > z} d^2\mathbf{b} dz dz' e^{iq_{\parallel}(z-z')} \rho^{(2)}(\mathbf{b}, z, z').$$

Here we have written explicitly only the first and the second terms in the expansion. The first term accounts for the incoherent scattering from bound nucleons while the second one is a correction due to the double scattering. The dots denote higher order scattering terms. The notations are as follows: $k = (k_0, \mathbf{0}_{\perp}, k_z)$ is the momentum of incoming off-shell (anti)quark, $q_{\parallel} = (m_q^2 - k^2)/2|k_z|$ is the longitudinal momentum transfer in the scattering of the (anti)quark from the nucleon, $t = -q_{\parallel}^2$, s is the (anti)quark-nucleon center-of-mass energy squared and $\rho^{(2)}(\mathbf{b}, z, z')$ is the two-nucleon density matrix. In our estimates we neglect effects due to inelastic excitations of the projectile particle in intermediate states as well as the effects of nucleon-nucleon correlations in the nucleus and assume that $\rho^{(2)}$ factorizes into two one-particle densities normalized to the unity, $\rho^{(2)}(\mathbf{b}, z, z') = \rho(\mathbf{b}, z)\rho(\mathbf{b}, z')$. In the numerical evaluations we use the Gaussian shape for the densities $\rho(\mathbf{b}, z)$ with the scale parameter fixed by the nuclear root-mean-square radius.

We use Eq.(10) to calculate (anti)quark-nuclear scattering amplitudes and then evaluate nuclear corrections to the quark $q(x)$ and antiquark $\bar{q}(x)$ parton distributions in the isoscalar nucleon by Eqs.(7,8). We keep the terms up to the 4th-order in the multiple scattering series (10). In Fig.3 we plot the ratios $R_2 = F_2^A/AF_2^N$ and $R_3 = F_3^A/AF_3^N$ for the calcium nucleus for the structure functions averaged over neutrino and antineutrino fluxes, $F_2 = (F_2^{\nu} + F_2^{\bar{\nu}})/2$ and $F_3 = (F_3^{\nu} + F_3^{\bar{\nu}})/2$ (the structure functions are evaluated for the isoscalar nucleon). The double scattering correction is negative⁵ and brings the main contribution to the multiple scattering series. However the share of the 3d-order and the 4th-order terms is also sizable, about 25% of the double scattering term in F_3 and about 15% in the case of F_2 for the calcium nucleus. The sum of the 3d-order and the 4th-order terms is positive and partially compensates the double scattering term. Note also that the share of higher order terms increases in heavy nuclei.

One can observe from Fig.3 that the nuclear shadowing effect for F_3 (i.e. for the valence quarks) is about 2 times stronger as the one for F_2 (i.e. for the sea quarks). To clarify the underlying reason for this factor of 2 we recall that the structure functions F_2 and F_3 are determined by the sum and by the difference of the antiquark and the quark scattering amplitudes respectively. At high energy the Pomeron pole dominates both the quark and the antiquark scattering amplitudes. The difference of the amplitudes, which

⁵ This is well seen from Eq.(10) if we neglect the effect of q_{\parallel} as well as a small real part of the scattering amplitudes.

is determined by the ω -Reggeon contribution, is small as compared to their sum. Since the double scattering correction in Eq.(10) is bilinear in the quark amplitude, we observe immediately that the relative correction to the difference of the quark and the antiquark cross sections is two times as bigger as the corresponding correction to their sum.⁶

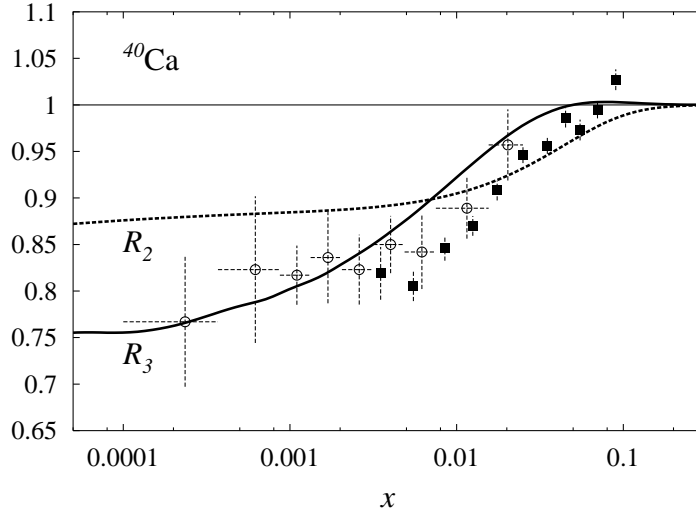


FIG.3

Ratios R_2 and R_3 calculated for the ^{40}Ca nucleus for small x and fixed $Q^2 = 5 \text{ GeV}^2$ (see text). The data points for the ratio R_2^μ are from NMC [1] (filled boxes) and E665 [2] (open circles) experiments with muon beams.

We found a sizable correction to the Gross-Llewellyn-Smith sum rule for heavy nuclei due to nuclear shadowing. For the calcium and iron nuclei the corrections are

$$\int_{10^{-5}}^{0.3} dx \left(\frac{1}{A} F_3^A(x) - F_3^N(x) \right) \approx \begin{array}{l} -0.11 \text{ } (^{40}\text{Ca}) \\ -0.12 \text{ } (^{56}\text{Fe}) \end{array} .$$

It is usually believed that the GLS sum rule should not be renormalized by nuclear effects in the leading in $1/Q^2$ order, because in this order the GLS integral counts the baryon number of the target. It is challenging therefore to look for a mechanism which would compensate a negative correction due to nuclear shadowing ('antishadowing'). Such an antishadowing may come from $x > 0.1$ region. We note in this respect that the Fermi-motion and nuclear binding corrections, which are of importance at large x , do not violate the GLS sum rule [12]. A possible 'compensating correction' could be due to off-shell modification of the bound nucleon structure functions.

In Fig.3 for comparison we put also the data points for R_2^μ for ^{40}Ca nucleus from NMC [1] and E665 [2] experiments with muon beams. We note that data is taken for different Q^2 for every x -bin and, due to the nature of the fixed target experiments, small x is always correlated with small Q^2 (for events with $x < 10^{-2}$ presented in Fig.3, averaged $Q^2 < 1 \text{ GeV}^2$). In the small Q^2 region where scaling is violated, the applicability of the leading twist calculation is questionable. We therefore need a model which provides a smooth transition from scaling to nonscaling region. In [6] we have considered a model which

⁶ The author is grateful to N. N. Nikolaev for useful discussion on this point.

interpolates the structure function F_2^μ (measured in muon induced reactions) between scaling and nonscaling regime where the latter was described in terms of vector meson dominance model [13] (VMD). It was found in the framework of this two “phase model” that the VMD part of F_2 is shadowed strongly than its scaling part. This lead to the enhancement of the overall nuclear shadowing effect. A similar observation has been done in a recent analysis of nuclear shadowing effect in neutrino induced DIS [14]. In conclusion we notice the importance of a small Q^2 analysis for the structure function F_3 . We recall in this respect that F_3 describes the axial-vector–vector current transitions in the target under the charged current and the studies of this effect may bring new insights into the problem of chiral symmetry violation in nuclear environment.

The author is grateful to W. Melnitchouk and N. N. Nikolaev for useful discussions and to the organizers of the Seminar for warm hospitality.

This work is supported in part by the RFBR grant 96-02-18897.

References

- [1] NMC Collab., P. Amaudruz *et al.*, Z. Phys. **C51**, 387 (1991); Z. Phys. **C53**, 73 (1992); M. Arneodo *et al.*, Nucl Phys. **B441**, 12 (1995).
- [2] E665 Collab., M. R. Adams *et al.*, Phys. Rev. Lett. **68**, 3266 (1992); Phys. Lett. **B287**, 375 (1992); Z. Phys. **C67**, 403 (1995).
- [3] R. J. M. Covolan, and E. Predazzi, in *Hadronic Physics With Multi-GeV Electrons, Les Houches, 1990*, eds. B. Desplanques and D. Goutte (Nova Science Publishers, N.Y., 1990); M. Arneodo, Phys. Rep. **240**, 301 (1994).
- [4] B. L. Ioffe, V. A. Khoze, and L. N. Lipatov, *Hard processes: Phenomenology, Quark-Parton Model* (Elsevier Science Publishers, North Holland, 1984).
- [5] P. V. Landshoff, J. C. Polkinghorne, and R. D. Short, Nucl. Phys. **B28**, 225 (1971).
- [6] S. A. Kulagin, G. Piller, and W. Weise, Phys. Rev. **C50**, 1154 (1994).
- [7] S. A. Kulagin, W. Melnitchouk, T. Weigl, and W. Weise, Nucl. Phys. **A597**, 515 (1996).
- [8] P. D. B. Collins, *Regge Theory and High-Energy Physics* (Cambridge Univ. Press, Cambridge, 1977).
- [9] A. Donnachie, and P. V. Landshoff, Phys. Lett. **B296**, 227 (1992).
- [10] R. J. Glauber, in *Lectures in Theoretical Physics*, ed. W. E. Brittin *et al.* (Interscience, N.Y., 1959).
- [11] V. N. Gribov, ZhETF **57**, 1306 (1969) [Sov. Phys. JETP **30**, 709 (1970)].
- [12] S. A. Kulagin, Nucl. Phys. **A640**, 435 (1998); e-print nucl-th/9801039.
- [13] G. Piller, and W. Weise, Phys. Rev. **C42**, 1834 (1990).
- [14] C. Boros, J. T. Londergan, and A. W. Thomas, e-print hep-ph/9804410.